

Simulation and experimental validation of fatigue endurance limit of copper alloy for industrial applications

M. Viscardi, P. Napolitano and M. Arena

Abstract— Fatigue resistance performance represents one of the main characteristic for flexible structures as those used in aerospace and other means of transport. For this reason, particular attentions are dedicated during the design stage to the evaluation of the lifetime resistance parameters. Many numerical and analytical approaches are actually available for this purpose, as well-standardized experimental test procedures have been assessed. With reference to a copper bar of an electric motor, the paper presents a survey of the main analytical and numerical methodologies for the prediction of the fatigue peculiarities. The estimation data have been then validated by an experimental campaign in simulated operating conditions, revealing advantage and drawbacks of different models.

Keywords— Fatigue analytical models, fatigue tests, Finite Element Model, mechanical fatigue, S-N curve.

I. INTRODUCTION

IN modern engineering field, the fatigue is one of the most relievable target to center for durability structures. The term fatigue was introduced for the first time in middle of the nineteenth century, when several railroad accidents drew the attention on the subject. Even today, the majority of all structures failures are attributed to fatigue stress, which means that dimensioning against fatigue is of utmost importance. In the aircraft sector, a significative observance to this topic has been given following the accidents involving the Comet G-ALYP and G-ALYY series in the 50's, caused by the fatigue failure of fuselage [1]. A total of 306 fatal accidents since 1934 were identified as having metal fatigue as a related cause, and these accidents resulted in 1803 fatalities [2]. After an overview on the metals fatigue concept with its historical empirical prediction criteria, the main results following an innovative experimental way on two different copper bars of the rotor cage of electric motors are outlined and described. The samples used, in particular, are constituted by a CuCrZr-F37 alloy type, which there are no detailed experimental characterizations yet. All testing activities have been carried out in the Department of Industrial Engineering (Aerospace Section, Università degli Studi di Napoli "Federico II"). Furthermore, the authors focused on the numerical simulation of the fatigue failure within COMSOL Multiphysics® in which several strain-based methods have been compared in terms of accuracy and compliance with the laboratory outcomes [16-17]. Thanks to this methodological approach, the benefits but also the technical aspects to be in-depth explored for careful results confidence have been underlined, showing the

imprecision to implement a too simplified model to analyze a complex physical phenomenon but at same time the utility in a preliminary research project stage.

II. FATIGUE IN STRUCTURES

The term fatigue is used to describe a particular failure type in a structure due to a repeated loading and unloading, even though the magnitude of every cycle is less than the ultimate stress of the material. The fatigue failure follows a precise scheme divided into three steps. In the first step, damage is accumulated in micro-mechanical scale. Some imperfections in material or some zones with an intensification of stress cause the presence and the growth of a micro fracture. The second step is the propagation one: this is also the longest period in fatigue life. The cracks inside the structure becomes macroscopic. Griffith leded the first studies on fragile material behavior in this phase [5]. After Griffith, Irwin and Orowan extended the investigation to plastic material and this is nowadays the common used method for fatigue assessment. During every cycle the crack grows leaving on the structure the typical "beach marks", Fig. 1. The third steps is the failure of the structures. Usually it happen when the resistant section is too small for applied loads.

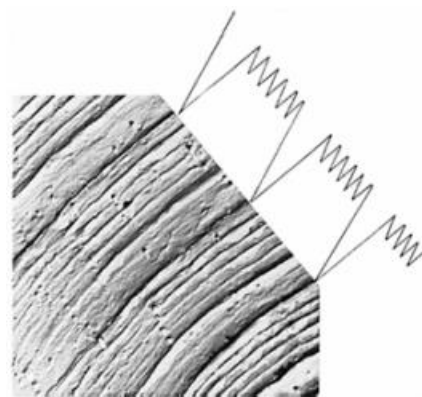


Fig. 1 Typical marks on a fatigued sample section

A. S-N curves

Wöhler, using a simple load cycle with amplitude and mean value constant in time, performed the first study on fatigue behavior of simple structures. The result of this operation is the S-N curves envelope that correlates the applied stress on test specimen and the number of cycles before failure, Fig. 2.

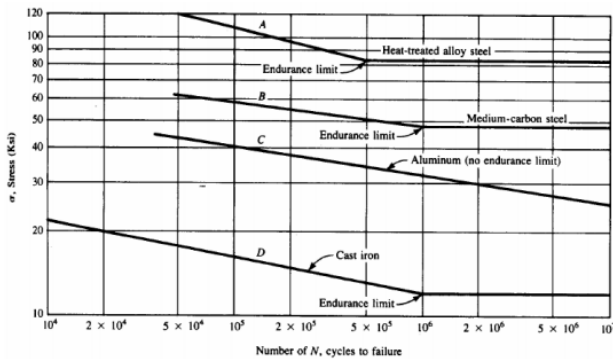


Fig. 2 S-N curves

One of the most relevant outcomes achieved by Wöhler was the introduction of “fatigue endurance limit” for some steel, non-iron alloy and titanium coincident with a change in slope of S-N curve (knee) [3]. The fatigue endurance limit is defined as the maximum stress capable for structure without it fails for fatigue. For other metals like iron alloy, aluminum this limit is a pseudo-limit and the fatigue endurance limit is the stress that gives a fatigue life upper than 10⁸ cycles, Fig. 3.

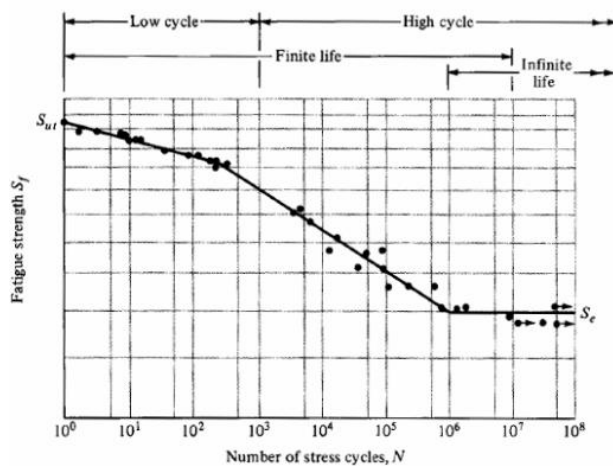


Fig. 3 S-N curve with variable load

In Fig. 3, the S-N curve is obtained reducing the stress amplitude from the maximum value (1 cycle failure) to the fatigue endurance limit. In particular, three functional zones can be distinguished. The first is called LCF (Low Cycle Fatigue) followed by the HCF (High Cycle Fatigue). The LCF covers the first 103 cycle, the HCF is the zone over 105 cycles. The area between 103 and 105 is a transition area and can be identified by a change in S-N curve slope. In LCF, the material behavior is plastic and the failure is related to the stress, while in HCF the material response is elastic and the failure is caused by the strain [4], [7]. The second change in slope close to 10⁸ cycles divides the finite life zone from the infinite life one. The S-N curves were extrapolated by Wöhler followed in-depth empirical investigations on different specimens. Two different models have been developed to reproduce the S-N curve. The first model is applied in LCF zone and is the Coffin-Manson model governed by the relationship (1):

$$\frac{\Delta \epsilon_p}{2} = \epsilon_f' (2N_f)^c \tag{1}$$

where compare the plastic strain range $\Delta \epsilon_p$, the cycles to failure $2N_f$, ϵ_f' and c represent indeed respectively the fatigue ductility coefficient and fatigue ductility exponent which depend from material properties.

The model for HCF zone was developed by Basquin and is expressed as:

$$\sigma_a = \sigma_f' (2N_f)^b \tag{2}$$

where $2N_f$ are the cycles to failure at a fixed stress level σ_a , while σ_f' and b are two material parameters.

The problem solution gets out by combining the two curves, Fig. 4, in a final analytical model capable to cover the LCF and HCF (3):

$$\frac{\Delta \epsilon}{2} = \frac{\sigma_f'}{E} (2N_f)^b + \epsilon_f' (2N_f)^c \tag{3}$$

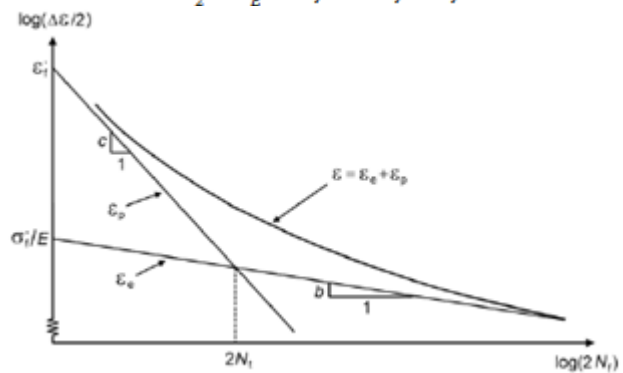


Fig. 4 S-N analytical curve

B. Load cycle definition

The typical load cycle shown in Fig. 5 can be identified by the parameters below:

- Stress amplitude:

$$\sigma_a = \frac{\sigma_{max} - \sigma_{min}}{2} \tag{4}$$

- Stress range:

$$\Delta \sigma = \sigma_{max} - \sigma_{min} \tag{5}$$

- Mean stress:

$$\sigma_m = \frac{\sigma_{max} + \sigma_{min}}{2} \tag{6}$$

- R value:

$$R = \frac{\sigma_{min}}{\sigma_{max}} \tag{7}$$

The parameter R is widely adopted to characterize the cycle type. In particular the most commonly used cycles are the “fully reversed cycle” ($R = -1$) and the “repeated cycle” ($R = 0$), Fig. 6.

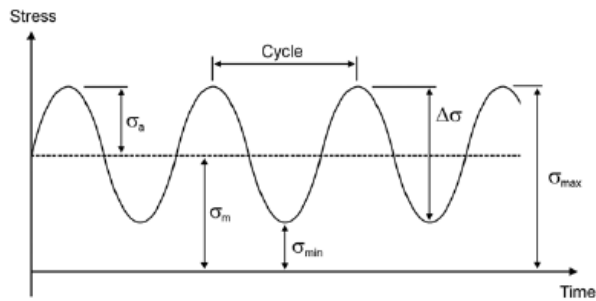
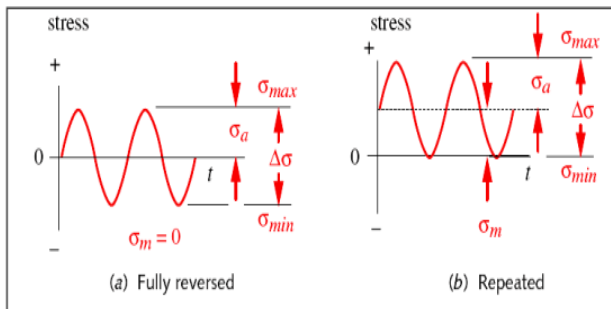


Fig. 5 Loading cycle example

Fig. 6 Most common cycles: $R = -1$ (a), $R = 0$ (b)

III. EXPERIMENTAL TEST

A. First approach: tensile stress test

The fatigue test of the material under investigation was initially conducted on mono-axial machine METROCOM[®] where frequencies with level excitation of the order of 1.2 Hz varied the intensity of the applied loads. The fatigue tests were carried out to estimate the fatigue life of the bar, by the formulation of an S-N curve. The tests were performed by imposing a traction load cycle, which ranges from about zero to a maximum load, were selected at the discretion of the operator taking into account the limits of elasticity, previously calculated. It was applied a sinusoidal signal divided into 16 steps, which constitute a complete load cycle. The first tests were conducted applying a cycle of 16 load steps from 0 to a maximum of 2350 Kg, so as to have 250 N/mm², being so widely in the linear elastic regime; after 135000 cycles (i.e. 37.5 hours of test) the test has not succeeded in breaking. In the second test, a cycle of 16 load steps was applied from 0 to a maximum of 2750 Kg, so as to have 290 N/mm², the specimen was broken at 2187 cycles, after 35000 cycles. The third test, finally, was conducted with an average load between the first two, 16 load steps from 0 to a maximum of 2600 Kg, thus having 275 N/mm². The specimen in this case still did not succeed in breaking and the test was stopped after 135000 cycles. The frequencies of operation allowed for leading to a non-viability of this methodology for the determination of the fatigue life of the specimen; the data obtained from these tests, however, confirmed the typical values found in the bibliography, in terms of the shape of Wöhler curve (S-N diagram). The operation mode of the bar, in the real application also provides a deformation in bending (or rather flexed torsion) and not in tension, such as the classic fatigue tests are conducted. In the next step, it was then engineered an

alternative methodology that would direct the test engineer to achieve, in acceptable times of work, a resistance test to flexural fatigue loading. This test differs from the classical way aimed at tracing the curve of Wöhler, because it does not seek the law relationships between load and fatigue cycles, but it intends to evaluate the ability of resistance over time at a given load, trying to make very similar the exercise load.

B. Alternative methodology: flexural fatigue test

For the test accomplishment, it was realized an alternative system in which the forcing is provided by one electro-dynamic shaker placed in order to excite the specimen flexurally fixed to a suitable strong-back constraint system, Fig. 7, 8. This set-up has been tried to reproduce the real operating environment of the bars in the rotor. The Fig. 9 shows the bar design details.

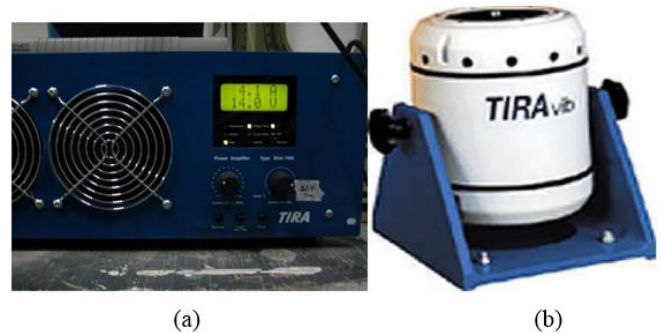


Fig. 7 Test instrumentation: amplifactory (a), shaker (b)

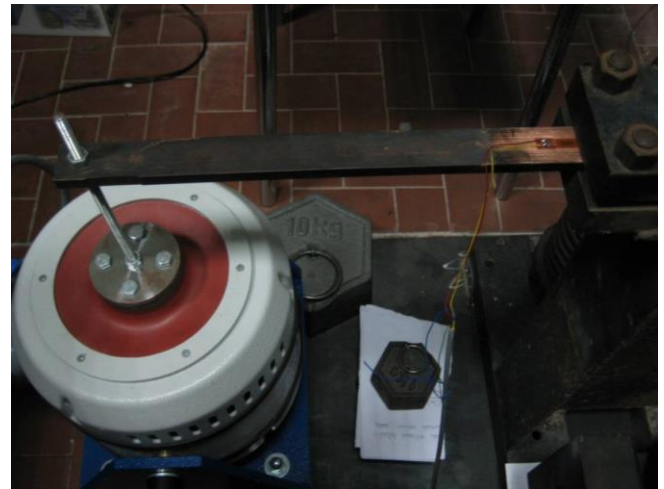


Fig. 8 Test set-up

The first survey implemented in the described set-up involved the analysis of the dynamic characteristics of the bar in standard sizes.

An ODS (Operation Deflection Shapes) analysis on bar, which velocity FFT (Fast Fourier Transform) is shown in Fig. 10, has been carried out by means of scanning Laser Doppler Vibrometer (LDV), Polytec 400[®] [6], [8], [18]. The initial

purpose was to be able to provide a displacement of 35 μm to simulate the real operating conditions of the bar inside the electrical motor. Exploiting the resonance of the system to 838 Hz, a sinusoidal signal at that frequency has been generated modulating the amplitude until it was acquired in the section of interest the displacement attempted.

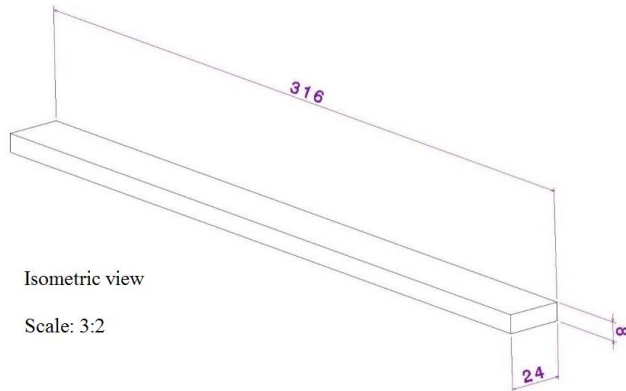


Fig. 9 Bar in standard size

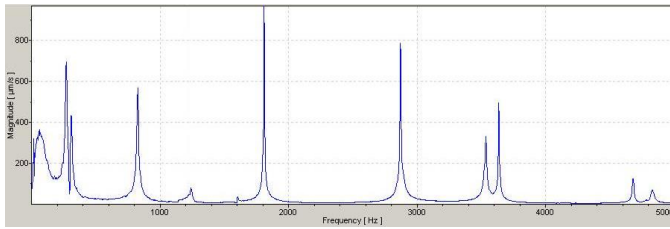


Fig. 10 Velocity FFT acquisition, Laser test

Relying upon the selected stress conditions it proceeded with the fatigue test: the reading of the strain gauges was carried out every two hours. The remarkable outcome was that the value of deformation measured has unchanged for the duration of the test, which was stopped after 150 hours without any impended failure of the sample. In total, a number of load cycles equal to $4.224 \cdot 10^8$ has been applied to the bar with an equivalent force applied by the shaker extreme stringer of about 13 N.

However, the specimen was changed, halving the thickness and reducing the length of the overhang to 40 mm according to a more conservative condition, Fig. 11.

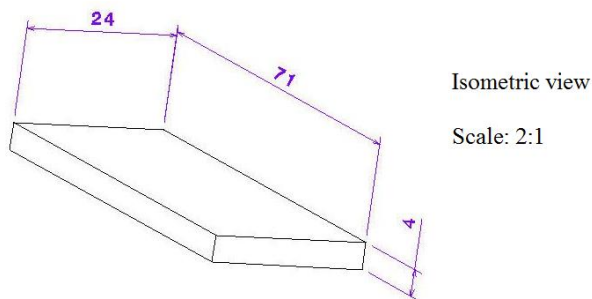


Fig. 11 The sample reduced in size

The thickness halving was dictated by the need to increase the maximum effort exercisable with the same shaker load as well as the overhang length reduction in order to have the best race

of the actuator: this arrangement allowed a greater elongation in the section of extensometer. In addition to experimental tests carried out on the new set-up, the maximum deformation measured from extensometer in different stress conditions has been analyzed. Starting from the interpolation of the strain values measured in relation to the frequency of the sinusoidal signal generated, the system showed a resonance at about 110 Hz. The specimen has been resized allowing the application of a greater load from the shaker; so a sinusoidal signal is generated at a frequency of 110 Hz because of the above rational considerations, with a power supply voltage of 2.5 Vpp. In such conditions, the load power provided by the shaker is equal to 304 N, for a tension snaps amounting to 190 N/mm². The value of the load provided by the shaker was implicitly evaluated being known the values of Young's modulus and the deformation acquired by the strain gauge, according to the classical methodology below callback, Fig. 12.

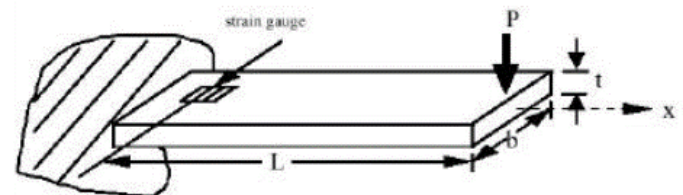


Fig. 12 Cantilever beam with strain gauge mounted on top

When a load (P) is applied at the free-tip of the beam, the tractive effort (σ) along the x-axis on the upper surface is given by:

$$\sigma = \frac{M * c}{I} \quad (8)$$

where:

- M is the bending moment as product of the actual beam length and the force P;
- c is the distance from the beam neutral axis (m). Typically $c = t / 2$, in which t is the thickness of the beam;
- I is the moment of inertia for a cross section of the beam (in units m⁴);
- L is effective length of the beam as distance between the load application point and the strain gauge center (m);
- b is the beam width (m).

In such load conditions, the sample was completely broken after 60 minutes corresponding to 396000 cycles, Fig. 13. It can be noticed that already after 30 minutes a fracture developed in the upper part of the sample, Fig. 14-15.

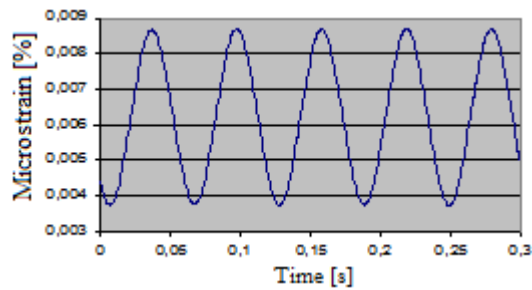


Fig. 13 Strain gauge reading after 5 minutes

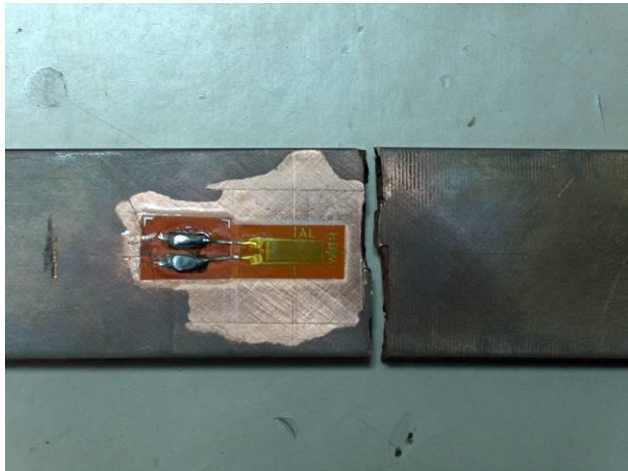


Fig. 14 Details of broken sample, upper view

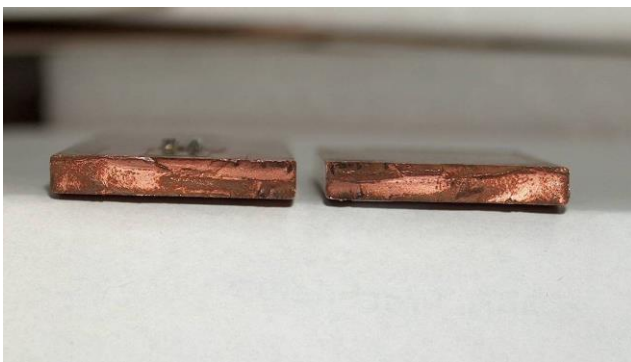


Fig. 15 Details of broken sample, section view

On a sample of the same dimensions of the previous one, it has generated a sinusoidal signal at the frequency of 110 Hz with a supply voltage of 1.8 Vpp; in such feeding conditions the load provided by the shaker amounts to 192 N, for a voltage snaps equal to 120 N/mm². The sample is broken completely after 64 hours for a number of cycles equal to $2.5 \cdot 10^7$.

In Fig. 16, 17 the details of the second sample arrived at break are well represented.

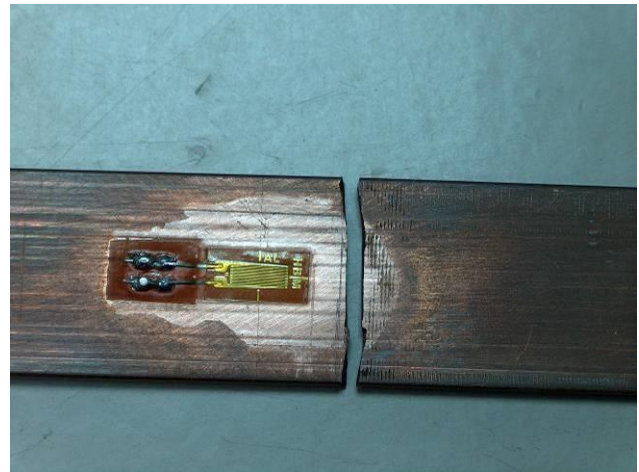


Fig. 16 Sample going to break, upper view



Fig. 17 Details section

C. Test conclusions

All conditions of load and number of cycles achieved can be summarized in the Table I.

At the end it can observe that:

- Voltage values expected for the exercise (based on data measured during the bar exercise) theoretically should never experience a fatigue failure, or at least for numbers of cycles greater than $10^9 - 10^{10}$;
- Copper, however, does not have an asymptotic behavior and the S-N curve shows a not negligible slope; small changes in the stress state can produce significant lowering of the number of cycles to fatigue, Fig. 18;
- The residual stresses that are going to generate during brazing can significantly change the stress state and reduce the total number of useful cycles;
- A last consideration concerns any micro-damages that may be created during the processing steps. These can greatly reduce the fatigue strength of components and lead to a premature failure.

Table I. Experimental test summary

Set-up	Tension snaps σ [N/mm ²]	Cycles	Result
Metrocom	275	$1.35 \cdot 10^5$	no break
Metrocom	250	$1.35 \cdot 10^5$	no break

Metrocom	290	$2.19 \cdot 10^3$	break
Shaker	190	$3.96 \cdot 10^5$	break
Shaker	120	$2.53 \cdot 10^7$	break
Shaker	17	$4.53 \cdot 10^8$	no break

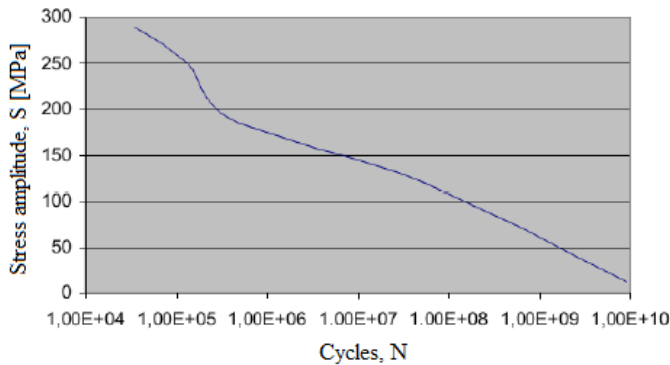


Fig. 18 S-N synthetic diagram

IV. NUMERICAL MODEL

The greater difficulty in simulate the fatigue behavior for structures is due to the high non-linearity of the problem [9]. Some shortcuts can be used to linearize the equations that govern the problem but often this approximation is unable to accord numerical results and experimental ones. The next steps are the development of a FE (Finite Element) model fully representative of the 3D cantilever beam under investigation, and performing a fatigue analysis by means of a multiphysics software. The fatigue analysis will be divided into two steps. In the first step, a load cycle will be simulated and in the second step, the result of first one will be used for fatigue life calculation.

The model has considered as solid material and its schematization is shown in Fig. 19.

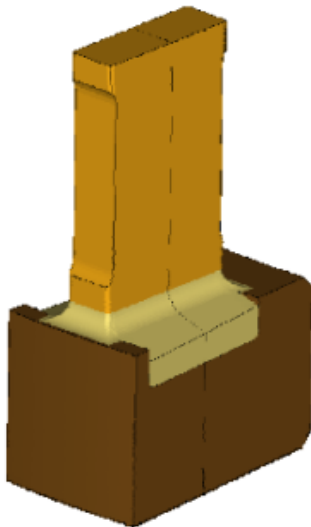


Fig. 19 3D CAD geometry

A fixed-free constraint has been selected according to simulate the real test condition. The fixed-end of the beam has constrained in all six degree of freedom. The load has been applied along the vertical direction to the free-end: this condition is really close to the real one. The geometry under investigation has two transversal surfaces very large respect to the cross section. To ensure a good mesh quality, the upper surfaces have been meshed with triangular elements and then swept along the short edge. The mesh consists of more than 37000 nodes and 2000 elements with an average quality of 0.34. The material used is copper with less than 1% of impurity which main mechanical properties are listed in Table II.

Table II Material general properties

Elastic modulus, E [GPa]	94
Poisson ratio, ν	0.355
Shear Modulus, G [GPa]	48
Density, ρ [Kg/m ³]	8920
Yield strength, σ_y [MPa]	278
Tangential Modulus, τ [MPa]	765.875

The fatigue models requires some other parameters that can be founded with experimental tests for the material characterization [11-13].

The parameters implemented, according to the strain-based fatigue models, are detailed below [16-17]:

- SWT model:
ductility coefficient, ductility exponent, strength coefficient and strength exponent;
- Wang-Brown model:
normal strain sensitivity coefficient;
- Fatemi-Socie model:
normal strain sensitivity coefficient.

Moreover, relatively to a HCF analysis, the stress-based models are known in which the parameters are normal stress sensitivity factor and the limit factor.

The cited method have been used to calculate the cycles to failure of the cantilever beam.

In the Table III, the numerical results are compared with the experimental ones while the usage factor for LCF models are indicated in the Table IV.

Table III HCF results comparison

	$\sigma = 120 \text{ N/mm}^2$	$\sigma = 190 \text{ N/mm}^2$
Experimental	$2.53 \cdot 10^7$	$3.95 \cdot 10^5$
SWT	$2.54 \cdot 10^7$	$4.13 \cdot 10^5$
Wang-Brown	$2.53 \cdot 10^7$	$4.17 \cdot 10^5$
Fatemi-Socie	$2.54 \cdot 10^7$	$2.37 \cdot 10^4$

Table IV Fatigue Usage Factor

	Fatigue Usage Factor (FUS)
Findley	5.46

Matake	5.36
Normal Stress	5.5

V. CONCLUSIONS

The mechanical components are often subject to stresses that vary cyclically over time, with an alternative succession of peaks and valleys in the loading history [14-15]. For example, the rotating members of the engines are subjected to periodic flexion loads due to the high rotation speeds. In this framework, the authors focused on the validation of a numerical model finalized to describe the fatigue behavior of a copper bar in several configurations. In ductile materials such as copper alloys, the failure is localized in the crystalline grains until to the total structural collapse. Experimental tests allowed for the deep investigating of the endurance capabilities under different cyclic loads; they were entirely conducted in the laboratory of Department of Industrial Engineering (Aerospace Section, Università degli Studi di Napoli "Federico II"). As shown in Table III – IV, the strain-based models have a good approximation for very high number of cycle becoming inadequate for LCF. The Fatemi-Socie model, in particular, is very poor in the neighbor of LCF zone. On the other side, the usage factor has been calculated with a good accordance between the three methods demonstrating the capabilities for these models to evaluate numerically the fatigue life for structures. Finally, it must highlighted that the structural arguments relating to pure copper or its alloys not so far found widespread knowledge and depth technical data since very rarely these materials are used with structural purposes; this lack is then even greater as regards the fatigue behavior. Another topic against which is not easy to gain actually bibliographic references or significant normative details is about the mechanical behavior of these materials subjected at high frequency vibrations, especially in the case of a drive motor rotor not easily assimilated to homogeneous elastic bodies. To overcome these uncertainties is therefore necessary to perform analytical checks and then integrated and validated by test evidence as well as by also innovative methods, such as to ensure a physical outcome with a greater accuracy than that one of a simple calculation model. Based on the results, any changes are suggested to prevent or control the non-repeatability of the adverse phenomenon. A potential further development will be to implement a rational approach for the analyzing the crack propagation with particular attention to the evaluation of residual stress as a cause of the fatigue life reduction of the mechanical component.

REFERENCES

- [1] P.A. Withey, "Fatigue failure of the de Havilland comet I," *Engineering Failure Analysis*, Vol.4, Issue 2, pp. 147-154, 1997.
- [2] G.S. Campbell, "A note on fatal aircraft accidents involving metal fatigue," *International Journal of Fatigue*, Vol. 3, pp. 181-185, 1981.
- [3] Wöhler, "English Abstract in Engineering," Vol 2, p. 199, 1871.
- [4] J. Goodman, "Mechanics Applied to Engineering," *Longmans, Green & Co.*, London, 1899.
- [5] A. A. Griffith, "The theory of rupture," *Proc. First Int. Conf. for Applied Mechanics*, Delft 1924. C.B. Biezeno and J.M. Burgers Eds., Waltman, Delft, 1925.
- [6] F. Ricci, M. Viscardi, "Dynamic behaviour of metallic and composite plates under in-plane loads," *Proceedings of the International Modal Analysis Conference - IMAC*, Vol. 1, pp. 99-103, 2000.
- [7] P.C. Paris and F. Erdogan, "A critical analysis of crack propagation laws," *Journal of Basic Engineering*, Vol. 85 528–534, 1963.
- [8] M. Viscardi, M. Arena, D. Siano, "Experimental and numerical assessment of innovative damping foams," *International Journal of Mechanics*, Vol. 10, pp. 329-335, 2016.
- [9] D. Roylance, "Mechanical properties of materials," pp. 37-40, 2008.
- [10] M. Viscardi, M. Iadevaia, L. Lecce, "Numerical/experimental characterization of a piezoelectric driven electromedical device," *14th International Congress on Sound and Vibration 2007, ICSV 14*, Vol. 3, pp. 2338-2345, 2007.
- [11] G. Scarselli, E. Castorini, F.W. Panella, R. Nobile, A. Maffezzoli, "Structural behaviour modelling of bolted joints in composite laminates subjected to cyclic loading," *Aerospace Science and Technology*, Vol. 43, pp. 89-95, 2015.
- [12] F. Ciampa, G. Scarselli, S. Pickering, M. Meo, "Nonlinear elastic wave tomography for the imaging of corrosion damage," *Ultrasonics*, Vol. 62, pp. 147-155, 2015.
- [13] G. Scarselli, L. Lecce, "Genetic algorithms for the evaluation of the mistune effects on turbomachine bladed disks," *ETC 2005 - 6th Conference on Turbomachinery: Fluid Dynamics and Thermodynamics*, 2005.
- [14] S.K. Bhaumik, M. Sujata, M.A. Venkataswamy, "Fatigue failure of aircraft components," *Engineering Failure Analysis*, Vol. 15, Issue 6, pp. 675-694, 2008.
- [15] D. Turan, A. Karci, "Failure analysis of an aircraft piston engine components," *Engineering Failure Analysis*, Vol. 16, Issue 4, pp. 1339-1345, 2008.
- [16] COMSOL, "Fatigue Model User's Guide," Ver. 4.4, 2013.
- [17] COMSOL, "Multiphysics Reference Manual," Ver. 4.3b, 2013.
- [18] M. Viscardi, M. Arena, "Experimental Characterization of Innovative Viscoelastic Foams," *Mechanics, Materials Science & Engineering*, Vol. 4, pp. 7-14, doi:10.13140/RG.2.1.5150.6325.

Massimo Viscardi was born in Naples (Italy) on the 28th of January 1970, where he graduated in Aerospace Engineering. Assistant professor of Aerospace Structural Testing and of Experimental Vibroacoustic at University of Naples, his research is mainly dedicated to innovative measurement and control technologies for acoustic and vibration phenomena. He has been involved in many EU project within the 6th, 7th framework as well H2020 contest.

Expert evaluator for the Ministry of Economic Development, Italy. He is member of several association and has been author of about 70 scientific papers as well as referee of many scientific journals.

Department of Industrial Engineering
Università degli Studi di Napoli "Federico II"
massimo.viscardi@unina.it

Maurizio Arena was born in Naples (Italy) on the 28th of December 1989, where he graduated in Aerospace Engineering. He is now involved in the Ph.D. program at University of Naples "Federico II", where he works within the Smart Structures group. His main area of interest are: smart structures, acoustic and vibration.

Department of Industrial Engineering
Università degli Studi di Napoli "Federico II"
maurizio.arena@unina.it